

## Measurement and Modeling of CO<sub>2</sub> Frost Points in the CO<sub>2</sub>–Methane Systems

Longman Zhang,<sup>†</sup> Rod Burgass,<sup>‡</sup> Antonin Chapoy,<sup>‡,\*</sup> Bahman Tohidi,<sup>‡</sup> and Even Solbraa<sup>§</sup>

<sup>†</sup>Norwegian University of Science and Technology, Department of Energy and Process Engineering, NO-7491 Trondheim, Norway

<sup>‡</sup>Centre for Gas Hydrate Research, Institute of Petroleum Engineering Heriot-Watt University, Edinburgh, EH14 4AS United Kingdom

<sup>§</sup>Statoil, Research and Development NO-7005 Trondheim, Norway

**ABSTRACT:** Technology is being developed to separate carbon dioxide (CO<sub>2</sub>) from natural gas by frosting CO<sub>2</sub> out from the mixture. Vapor–solid phase equilibrium data in the CO<sub>2</sub>–methane systems are important in developing such processes. In this work, new experimental data are reported for the frost points in the CO<sub>2</sub>–methane systems for a wide range of CO<sub>2</sub> range concentration (i.e., CO<sub>2</sub> mole fraction 0.108 to 0.542). The Soave–Redlich–Kwong (SRK) equation of state (EoS) is employed to calculate the fugacity of the fluid phase. The CO<sub>2</sub> solid-forming conditions are modeled by a solid fugacity model based on the sublimation pressure of pure CO<sub>2</sub>. The thermodynamic model was used to predict the CO<sub>2</sub> frost points in the presence of methane. Predictions of the developed model are validated against independent experimental data and the data generated in this work. A good agreement between predictions and experimental data is observed, supporting the reliability of the developed model.

### INTRODUCTION

Removal of CO<sub>2</sub> from high carbon dioxide (CO<sub>2</sub>) content natural gas fields is important to the gas industry development in some countries. For example, in Malaysia alone, over 13 Tscf of hydrocarbon gas remains undeveloped in high CO<sub>2</sub> content fields, where the CO<sub>2</sub> mole fraction is even higher than 0.70 in some gas fields.<sup>1</sup> One challenge in developing such gas fields is the economical separation of CO<sub>2</sub> from the feed gas. A technique has been suggested based on frosting CO<sub>2</sub> at low temperature and separating the CO<sub>2</sub> solid from the natural gas; hence, technologies are being developed to efficiently separate the CO<sub>2</sub> especially in high CO<sub>2</sub> content feed gases.<sup>2,3</sup> Therefore understanding of the vapor–solid equilibrium at low temperature is critical in designing such separation processes.

Existing experimental data on CO<sub>2</sub> frost from CO<sub>2</sub>–methane and other gas mixtures are scarce and normally focused on low CO<sub>2</sub> content systems. Pikaar<sup>4</sup> measured the frost points in CO<sub>2</sub>–methane systems for the (0.01 to 0.20) CO<sub>2</sub> mole fraction concentration range. Agrawal<sup>5</sup> measured the frost points in the CO<sub>2</sub>–N<sub>2</sub>–methane system for the (0.0012 to 0.1067) CO<sub>2</sub> mole fraction concentration range. More recently, Le<sup>6</sup> measured the frost points in CO<sub>2</sub>–methane, CO<sub>2</sub>–methane–N<sub>2</sub>, and CO<sub>2</sub>–methane–ethane systems for the (0.01 to 0.0293) CO<sub>2</sub> mole fraction concentration range.

In this work, the frost points have been measured in the CO<sub>2</sub>–methane systems for the CO<sub>2</sub> content of 0.108, 0.178, 0.334, 0.424, and 0.542 mol fraction, these data are important for evaluating thermodynamic models for process simulation. A thermodynamic model using the well-proven SRK equation of state<sup>7</sup> has been employed to model the phase equilibria. The thermodynamic model is based on uniformity of fugacity of each component throughout all the phases. The CO<sub>2</sub>–solid phase is modeled by a solid fugacity model based on the sublimation pressure of pure CO<sub>2</sub>. Experimental data both from this work and literature have been compared to the modeling work and good agreement between experimental data and predictions is observed.

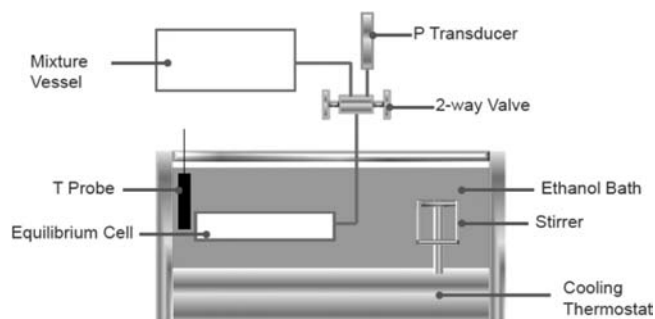


Figure 1. Schematic of the experimental apparatus.

### EXPERIMENTAL SECTION

The frost temperature is measured based on detecting CO<sub>2</sub> solid melting point during heating of a CO<sub>2</sub>–methane solid–vapor mixture in a constant volume equilibrium cell.

**Materials.** Ultra high pure grade methane (99.995 % pure) and CO<sub>2</sub> (99.99 % pure) supplied by BOC were used. Each synthetic mixture was made up by gravimetric means using the above pure components. The gas composition was checked using gas chromatography (GC). The GC (VARIAN model CP-3800) is equipped with two detectors in series, a thermal conductivity detector (TCD) and a flame ionization detector (FID). The TCD was used to detect CO<sub>2</sub>. It was repeatedly calibrated by introducing known amounts of CO<sub>2</sub> through a gas syringe in the injector of the gas chromatograph. The CO<sub>2</sub> calibration uncertainty is estimated to be within ± 0.8 %. The FID was used to detect methane and the same calibration procedure was used. The methane calibration uncertainty is estimated to be within ± 0.7 %.

Received: March 24, 2011

Accepted: May 12, 2011

Published: May 20, 2011

**Experimental Bath Apparatus.** Figure 1 shows the apparatus used for determining the frost points of the solid CO<sub>2</sub> in the CO<sub>2</sub>–methane mixture. The stainless steel equilibrium cell, which is approximately 11 mL in volume, is submerged in an ethanol bath. The temperature of the ethanol is controlled by a thermostat (LAUDA Proline RP 1290) with a working temperature range (183.15 to 323.15) K, the stability of the bath

**Table 1. Experimental and Predicted Frost Points in CO<sub>2</sub>–Methane (CO<sub>2</sub> Mole Fraction) Systems**

P, kPa	T, K (±0.32)		dev. <sup>a</sup> , K	∂P/∂T, kPa·K <sup>-1</sup>
	exp.	pred.		
CO <sub>2</sub> : 0.108 (±0.0017)				
2031(±16.5)	200.5	200.6	-0.1	14.1
4446(±22.4)	205.3	205.0	0.3	52.1
1342(±16.2)	197.5	196.6	0.8	8.4
CO <sub>2</sub> : 0.178 (±0.0028)				
2943(±17.4)	210.3	211.1	-0.8	22.7
1581(±16.3)	205.1	205.1	0.0	9.9
869(±16.1)	197.4	198.4	-1.0	5.1
497(±16.0)	191.1	192.2	-1.1	2.8
CO <sub>2</sub> : 0.334 (±0.0053)				
1144(±16.1)	209.5	210.4	-0.9	6.7
727(±16.0)	203.8	204.7	-0.9	4.1
572(±16.0)	202.6	201.8	0.8	3.1
448(±16.0)	199.5	198.8	0.7	2.4
307(±16.0)	194.2	194.3	-0.1	1.7
CO <sub>2</sub> : 0.424 (±0.0068)				
854(±16.0)	209.5	210.3	-0.8	2.5
478(±16.0)	202.5	202.8	-0.3	2.6
293(±16.0)	196.5	196.8	-0.3	1.6
CO <sub>2</sub> : 0.542 (±0.0087)				
568(±16.0)	209.1	208.5	0.6	3.1
329(±16.0)	202.7	201.4	1.3	1.8

<sup>a</sup>Dev. = exp. - pred.

temperature is ± 0.02 K. The ethanol is stirred continuously to maintain a homogeneous temperature distribution in the bath.

The equilibrium cell temperature is measured by a platinum resistance thermometer submerged in the ethanol bath. The temperature probe was calibrated against a *Prema* 3040 precision thermometer. The uncertainty of the temperature probe is 0.05 K. The equilibrium cell pressure is measured by a pressure transducer (Quartzdyne QS10K-B, pressure range (0 to 68947) kPa). The pressure transducer was calibrated regularly using a Budenberg dead weight tester. The uncertainty of the pressure transducer is ± 8 kPa. The temperature and pressure are recorded by a PC in 10 s intervals during the experiments.

**Experimental Procedures.** The experimental procedure can be divided into two steps: mixture preparation and frost point determination.

*Step 1: Mixture Preparation.* A high pressure piston vessel (volume 300 mL) with a mixing metal ball inside is used for mixture preparation. First the vessel is vacuumed and weighed using a balance with a precision of 0.01 g. Then the desired amount (by weighing the vessel) of CO<sub>2</sub> and methane are introduced into the vessel. After mixing CO<sub>2</sub> and methane in the vessel, the composition is checked using GC, the compositions of these mixtures are listed in Table 1. The pressure of the mixture is kept lower than its dew point at room temperature, so that the mixture stays single phase inside the vessel.

*Step 2: Frost Point Determination.* Prior to the tests, the equilibrium cell was cleaned and vacuumed, and then the prepared CO<sub>2</sub>–methane mixture was loaded into the equilibrium cell. Figure 2 demonstrates the temperature and pressure relationship during the process of frost-point determination in the mixture of CO<sub>2</sub> 0.334 mol fraction. The equilibrium cell is cooled to a temperature 3 K (212 K in Figure 2) higher than the estimated frost temperature (209 K in Figure 2) in 1 h. Then the equilibrium cell is cooled slowly to a temperature 8 K (201 K in Figure 2) below the estimated frost point in 6 h, and stepwise cooling with 1 K intervals is used near the frost temperature. (In Figure 2, the temperature is cooled to 211 K and held for 30 min and then cooled to 210 K in 30 min and held at 210 K for 30 min; then the same process is repeated at (209, 208, and 207) K.) After cooling, the mixture is slowly heated to 3 K above the estimated frost point in 10 h, and again, stepwise heating is used near the

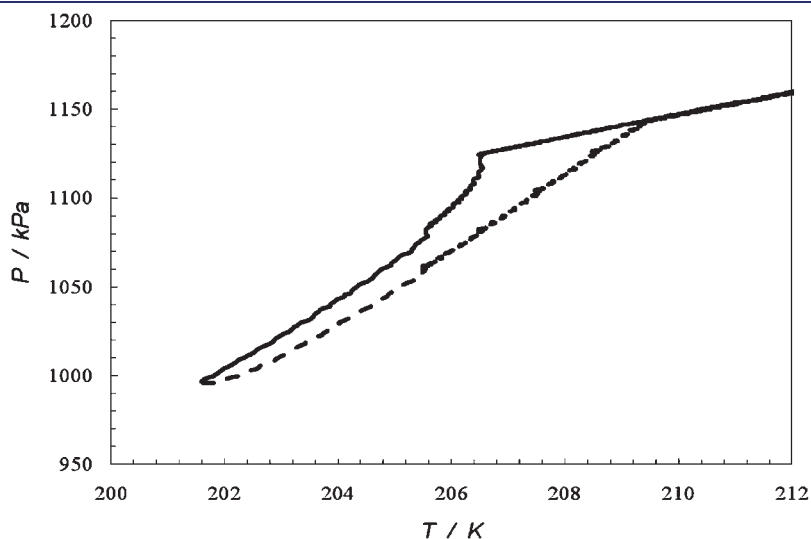


**Figure 2.** Frost point determination in the CO<sub>2</sub>–methane mixture (0.334 CO<sub>2</sub> mole fraction). Solid line: cooling process; dash line: heating process.

frost temperature. As demonstrated in Figure 2, this process results in two traces with very different slopes on a pressure versus temperature (PT) plot: one before and one after the frost

**Table 2. Parameters Used in the Calculation**<sup>10,11</sup>

	methane	CO <sub>2</sub>
$T_{\text{triple}}/\text{K}$	90.67	216.58
$P_{\text{triple}}/\text{kPa}$	11.7	514
$T_{\text{critical}}/\text{K}$	190.58	304.19
$P_{\text{critical}}/\text{kPa}$	4604	7382
acentric factor	0.0108	0.2276
enthalpy of sublimation/ $\text{kJ}\cdot\text{mol}^{-1}$		26.1
solid specific volume/ $\text{m}^3\cdot\text{mol}^{-1}$		$2.91 \times 10^{-5}$

point. The point where these two traces intersect (i.e., an abrupt change in the slope of the PT plot) is the temperature at which the CO<sub>2</sub> solid has totally melted, and this point is taken as the frost point. In this procedure, the standard deviation of the determined temperature is 0.15 K, and the uncertainty of the pressure is dependent on the temperature uncertainty.

**Thermodynamic Modeling and Correlation.** Calculations are based on equal fugacities of each component in different phases. For the vapor phase, the SRK EoS<sup>7</sup> with van der Waal mixing rule<sup>8</sup> is used to calculate the fugacities.

During the calculation, the solid phase is considered as a single pure component solid (CO<sub>2</sub> in this work). The solid phase fugacity is calculated by the following equation:<sup>9</sup>

$$f_{\text{CO}_2}^{\text{Solid}} = P_{\text{CO}_2}^{\text{Sub}} \varphi_{\text{CO}_2}^{\text{Sub}} e^{V_{\text{CO}_2}^{\text{Solid}}(P - P_{\text{CO}_2}^{\text{Sub}})/(RT)} \quad (1)$$

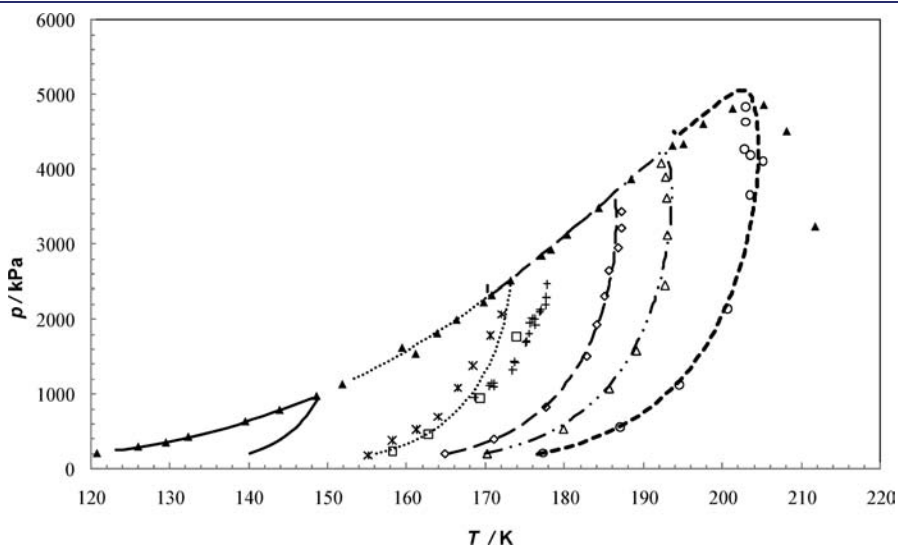


**Figure 3.** Correlation of CO<sub>2</sub> solid behavior in CO<sub>2</sub>–methane mixture (CO<sub>2</sub> mole fraction 0.01 to 0.10). Experimental data:  $\blacktriangle$ : 3 phase locus (Davis, 1962);<sup>13</sup>  $\circ$ : CO<sub>2</sub> 0.10 (Pikaar, 1959);<sup>4</sup>  $\triangle$ : CO<sub>2</sub> 0.05 (Pikaar, 1959);<sup>4</sup>  $\diamond$ : CO<sub>2</sub> 0.03 (Pikaar, 1959);<sup>4</sup>  $\square$ : CO<sub>2</sub> 0.01 (Pikaar, 1959);<sup>4</sup>  $*$ : CO<sub>2</sub> 0.0097 (Agrawal and Laverman, 1974);<sup>5</sup>  $+$ : CO<sub>2</sub> 0.01 (Le and Trebble, 2007).<sup>6</sup> Lines: Model correlations.

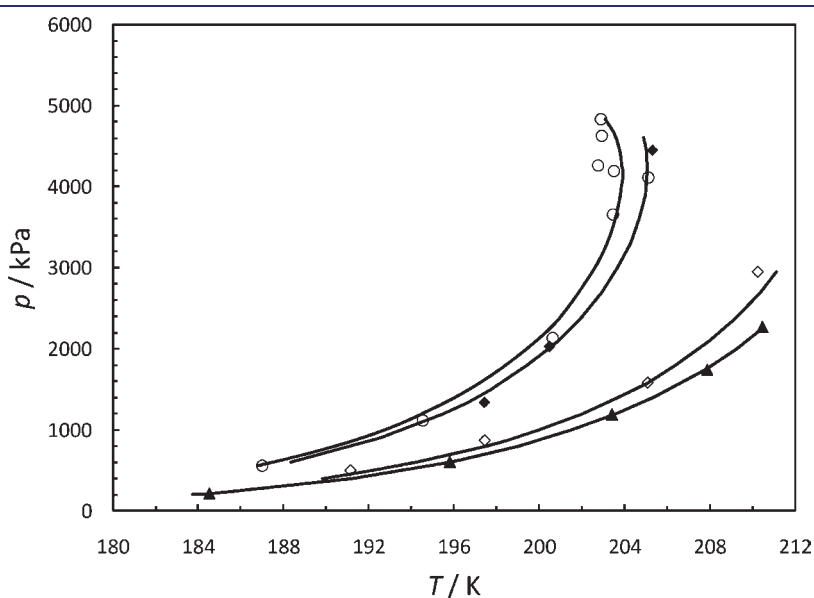


**Figure 4.** Frost points in the CO<sub>2</sub>–methane mixture (mole fraction,  $\circ$ : CO<sub>2</sub> 0.10 (Pikaar, 1959);<sup>4</sup>  $\blacktriangle$ : CO<sub>2</sub> 0.20 (Pikaar, 1959);<sup>4</sup>  $\blacklozenge$ : CO<sub>2</sub> 0.108 (this work);  $\diamond$ : CO<sub>2</sub> 0.178 (this work). Solid lines: Model prediction.

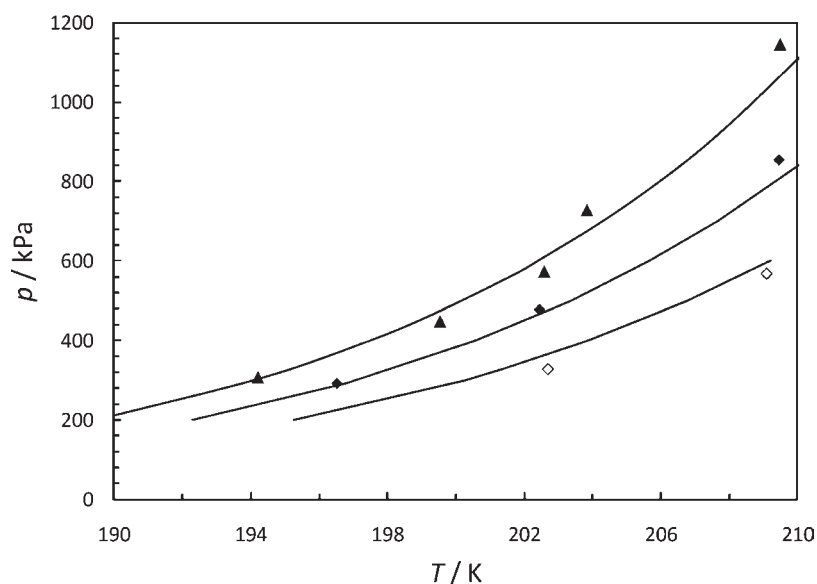


**Figure 5.** Frost points in the CO<sub>2</sub>–methane mixture. Mole fraction ▲: CO<sub>2</sub> 0.334; ◆: CO<sub>2</sub> 0.424; ◇: CO<sub>2</sub> 0.542. Solid lines: Model prediction.

where  $P_{\text{CO}_2}^{\text{Sub}}$  is the sublimation pressure of CO<sub>2</sub>,  $\varphi_{\text{CO}_2}^{\text{Sub}}$  is the fugacity coefficient of CO<sub>2</sub> at sublimation pressure at the system temperature  $T$ ,  $V_{\text{CO}_2}^{\text{Sub}}$  is the CO<sub>2</sub> solid specific volume at triple point temperature.

The assumption is made that solid can only form at temperature below the triple point temperature of CO<sub>2</sub>. The Clausius–Clapeyron equation is used to calculate the sublimation pressure:

$$\ln\left(\frac{P_2}{P_1}\right) = \left(\frac{\Delta_{\text{sub}}H}{R}\right)\left(\frac{1}{T_1} - \frac{1}{T_2}\right) \quad (2)$$

where  $\Delta_{\text{sub}}H$  is enthalpy of sublimation of CO<sub>2</sub> at triple point, and the triple point is set as the reference point. The parameters used in the calculation are listed in Table 2.

The same model was used by Zhang et al.<sup>12</sup> to correlate the binary interaction parameter for the SRK EOS according to the frost points in the CO<sub>2</sub>–methane system for a CO<sub>2</sub> concentration range of (0.0001 to 0.10) mole fraction, and the binary interaction parameter for SRK EOS is set as 0.12, which is the value used by Zhang et al.<sup>12</sup> Figure 3 shows the results of the model in correlating the SRK EOS binary interaction parameter by Zhang et al.<sup>12</sup>

## RESULT AND DISCUSSION

**Measured Frost Points and Uncertainty Analysis.** CO<sub>2</sub> frost points have been measured in the CO<sub>2</sub>–methane systems for a wide range of CO<sub>2</sub> concentrations (i.e., 0.108 to 0.542 mol fraction), and experimental results are listed in Table 1.

The frost temperature uncertainty sources considered in this work are uncertainty of the ethanol bath  $u_{T_{\text{bath}}} = 0.02$  K, uncertainty of the temperature probe  $u_{T_{\text{probe}}} = 0.05$  K, and the temperature standard deviation of the experimental procedure (Figure 2) in determining the frost temperature  $u_{T_{\text{loop}}} = 0.15$  K. The combined temperature standard uncertainty  $u_T$  is calculated as

$$u_T = \sqrt{u_{T_{\text{bath}}}^2 + u_{T_{\text{probe}}}^2 + u_{T_{\text{loop}}}^2} = 0.16 \text{ K} \quad (3)$$

A coverage factor  $k = 2$  is used in this work, and the expanded temperature uncertainty  $U_T$  with a confidence of 95 % is

$$U_T = ku_T = 0.32 \text{ K} \quad (4)$$

The frost pressure uncertainty sources considered in this work are uncertainty of the pressure transducer  $u_{P_{\text{transducer}}} = 8$  kPa and the pressure standard deviation of the experimental procedure (Figure 2)  $u_{P_{\text{loop}}}$  in determining the frost pressure. According to the Gibbs phase rule, the frost pressure determined in this work is dependent on the frost temperature, which could be expressed as  $P_{\text{frost}} = f(T_{\text{frost}})$ , so  $u_{P_{\text{loop}}}$  can be calculated by the following equation:

$$u_{P_{\text{loop}}} = u_{T_{\text{loop}}}\frac{\partial P}{\partial T} \quad (5)$$

The combined pressure standard deviation is calculated as

$$u_p = \sqrt{u_{P_{\text{transducer}}}^2 + u_{P_{\text{loop}}}^2} \quad (6)$$

The expanded pressure uncertainty  $U_p$  with a confidence of 95 % is

$$U_p = ku_p \quad (7)$$

$\partial P/\partial T$  in eq 5 is calculated by the NIST REFPROP<sup>14</sup> with the GERG-2004 EOS,<sup>15</sup> and the values are listed in Table 1. The expanded pressure uncertainties for each measure points are listed in Table 1.

The uncertainty source of concentration of the CO<sub>2</sub> in the mixture considered in this work is: uncertainty from the GC. The standard concentration deviation (mole fraction) of the CO<sub>2</sub>

$$u_{\text{CO}_2} = 0.8 \% y_{\text{CO}_2} \quad (8)$$

$y_{\text{CO}_2}$  is the mole fraction of CO<sub>2</sub>, and the expanded uncertainty of the CO<sub>2</sub> concentration with a 95 % confidence is

$$U_{\text{CO}_2} = ku_{\text{CO}_2} \quad (9)$$

**Comparison with Data from Selected Literature and Model Prediction.** The comparison of experimental data with

calculation from model are presented in Table 1 and plotted in Figures 4 and 5. The maximum temperature deviation is 1.3 K.

In this work, the comparison between experimental data (0.10 and 0.20 CO<sub>2</sub> mole fraction) obtained by Pikaar<sup>4</sup> and the model predictions are shown in Figure 4. The predictions of the developed model are compared against these independent experimental data and the data generated in this work over a wide range of temperature, pressure, and CO<sub>2</sub> concentration. A good agreement between predictions and experimental data is observed, demonstrating the reliability of the developed model.

## CONCLUSION

In this work new experimental data has been reported for the frost points of CO<sub>2</sub>–methane systems over a wide range of concentration (i.e., 0.108, 0.178, 0.334, 0.424, and 0.542 CO<sub>2</sub> mole fraction), temperature, and pressure.

The SRK equation of state has been applied to predict the frost point of these systems. The predictions of the developed model are compared against independent experimental data and the data generated in this work over a wide range of temperature, pressure, and CO<sub>2</sub> concentration. A good agreement between predictions and experimental data is observed, demonstrating the reliability of the developed model. The maximum temperature deviation between the model prediction and experimental data is 1.3 K.

## AUTHOR INFORMATION

### Corresponding Author

\*Phone: +44(0)1314 513797. Fax +44(0)1314 513 127. E-mail: antonin.chapoy@pet.hw.ac.uk.

### Funding Sources

This work was sponsored by the Norwegian Research Council through the (2007–2009) National Strategic Research Programme (Institusjonsforankret strategisk prosjekt (ISP)). The authors thank the Institute of Petroleum Engineering and Hydrofact Limited for providing support and experimental equipment for this work.

## REFERENCES

- (1) Darman, N. H.; Harum, A. R. B. *Technical Challenges and Solutions on Natural Gas Developmet in Malaysia*. In The petroleum Policy and Management Project, 4th Workshop of the China-Sichuan Basin Study, Beijing, China, 2006.
- (2) Hart, A.; Gnanendran, N. *Cryogenic CO<sub>2</sub> Capture in Natural Gas*; Energy Procedia, **2009**, *1*, 697-706.
- (3) Parker, M. E.; Valencia, J. A.; Foglesong, R. E.; Duncan, W. T. *CO<sub>2</sub> Management at ExxonMobil's LaBarge Field, Wyoming, USA*. In International Petroleum Technology Conference; Doha, Qatar, 2009.
- (4) Pikaar, M. J. *A Study of Phase Equilibria in Hydrocarbon-CO<sub>2</sub> Systems*, in Department of Chemical Engineering; Imperial College of Science and Technology: London, 1959.
- (5) Agrawal, G. M.; Laverman, R. J. Phase Behavior of the Methane Carbon Dioxide System in the Solid-Vapor Region. *Adv. Cryog. Eng.* **1974**, *19*, 317–338.
- (6) Le, T. T.; Trebble, M. A. Measurement of Carbon Dioxide Freezing in Mixtures of Methane, Ethane, and Nitrogen in the Solid-Vapor Equilibrium Region. *J. Chem. Eng. Data* **2007**, *52* (3), 683–686.
- (7) Soave, G. Equilibrium Constants from a Modified Redlich-Kwong Equation of State. *Chem. Eng. Sci.* **1972**, *27* (6), 1197–1203.

- (8) Kwak, T. Y.; Mansoori, G. A. Van der waals mixing rules for cubic equations of state. Applications for supercritical fluid extraction modeling. *Chem. Eng. Sci.* **1986**, *41* (5), 1303–1309.

- (9) Prausnitz, J. M.; Lichtenthaler, R. N.; Azevedo, E.G.d. *Molecular Thermodynamics of Fluid-Phase Equilibria*, 3rd ed.; Prentice-Hall, Inc.: NJ, 1999.

- (10) Daubert, T. E.; Danner, R. P. *Physical and Thermodynamic Properties of Pure Chemicals*; Design Institute for Physical Property Data, American Institute of Chemical Engineering, 1989.

- (11) NIST Chemistry WebBook. [cited 2011 Feb. 17]; <http://webbook.nist.gov/chemistry/>.

- (12) Zhang, L.; Solbraa, E. Prediction of Solid Fluid Phase Equilibrium in Gas Processing at Low Temperature, in 1st Trondheim Gas Technology Conference; Trondheim, Norway, 2009.

- (13) Davis, J. A.; Newell, R.; Fred, K. Solid-liquid-vapor phase behavior of the methane-carbon dioxide system. *AIChE J.* **1962**, *8* (4), 537–539.

- (14) Lemmon, E. W.; Huber, M. L.; McLinden, M. O. *NIST Standard Reference Database 23: Reference Fluid Thermodynamic and Transport Properties-REFPROP, Version 9.0*; Standard Reference Data Program; National Institute of Standards and Technology: Gaithersburg, MD, 2010.

- (15) Kunz, O.; Klimeck, R.; ; Wagner, W. *The GERG-2004 Wide-Range Equation of State for Natural Gases and Other Mixtures*; Groupe Européen de Recherches Gazières, 2007.